

Electric discharge contour dynamics model: the effects of curvature and finite conductivity on the velocity of propagation.

M. Arrayás¹ and M. A. Fontelos²

¹*Área de Electromagnetismo, Universidad Rey Juan Carlos,
Camino del Molino s/n, 28943 Fuenlabrada, Madrid, Spain and*

²*Instituto de Ciencias Matemáticas (CSIC-UAM-UCM-UC3M),
C/ Nicolás Cabrera, 28049 Madrid, Spain*

(Dated: February 13, 2019)

Abstract

In this paper we present the complete derivation of the effective contour model for electrical discharges which appears as the asymptotic limit of the minimal streamer model for the propagation of electric discharges, when the electron diffusion is small. It consists of two integro-differential equations defined at the boundary of the plasma region: one for the motion and a second equation for the net charge density at the interface. We have computed explicit solutions with cylindrical symmetry and found the dispersion relation for small symmetry-breaking perturbations in the case of finite resistivity. We implement a numerical procedure to solve our model in general situations. As a result we compute the dispersion relation for the cylindrical case and compare it with the analytical predictions.

PACS numbers: 51.50.+v, 52.80.-s

I. INTRODUCTION

The electrical breakdown of various media is usually caused by the appearance and propagation of ionization waves and, in particular, streamers. In the case of a gas, the specific features of the breakdown waves are determined by the type of the gas, the value of the pressure, the geometry of the discharge cell and the value and variation rate of the voltage at the electrodes. The geometry determines the space distribution of the electric field and hence the dynamics of the ionization fronts. In the case where there is no initial ionization in the discharge gap, the ionization wave may originate from one or several overlapping electron avalanches. After attenuation of the electric field in the avalanche body, a conducting channel or streamer develops: a plasma region fully ionized with a positive side expanding towards the cathode and a negative region towards the anode.

One of the approaches used to model the development of the avalanche-streamer transition and the streamer propagation is a nonlinear system of balance equations with a diffusion-drift approximation for the currents, together with Poisson equation [1]. Some progress in the understanding of the propagation mechanism has been achieved using that model. We can mention: the study of stationary plane ionization waves [2, 3], self-similar solutions for ionization waves in cylindrical and spherical geometries [5, 6], the effect of photoionization [7] and a branching mechanism as the result of the instability of planar ionization fronts [8–10]. In this hydrodynamic approximation, the fronts are subject to both stabilizing forces due to diffusion which tend to dampen out any disturbances, and destabilizing forces due to electric field which promote them. The solution of the model, even in the simplest cases, poses a challenging problem both numerical and analytical. Early numerical simulations can be found in [11, 12]. Recently, a contour dynamics model has been deduced in the limit of small electron diffusion [13], which resembles the Taylor-Melcher leaky dielectric model for electrolyte solutions [14], but adapted to the context of electric (plasma) discharges. This contour dynamics model allows to study more general situations in two-dimensional and three-dimensional cases.

The contour dynamics model consists of an interface separating a plasma region from a neutral region which evolves following the equation in dimensionless form

$$v_N = -E_\nu^+ + 2\sqrt{D\alpha(|E_\nu^+|)} - D\kappa, \quad (1)$$

where E_ν^+ is the normal component of the electric field at the interface when approaching

it from the region without plasma, D the diffusion coefficient, $\alpha(|E_\nu^+|)$ the Tonwsend term (5) and κ the curvature of the interface. At the interface, the total negative surface charge density changes according to

$$\frac{\partial\sigma}{\partial t} + \kappa v_N \sigma = -\frac{E_\nu^-}{\varrho} - j_\nu^-, \quad (2)$$

being now E_ν^- the electric field at the interface coming from inside the plasma, ϱ is a dimensionless parameter proportional to the resistivity of the plasma and j_ν^- the current contribution of any electromotive force if present.

In this paper, using the contour dynamics model, we will study cylindrical discharges when the plasma created has finite conductivity. The dispersion curve for transversal instabilities will be obtained for these finite conductivity streamers. The results will be compared with the limiting cases of perfect conductivity, which is the Lozansky-Firsov model [15] with a correction due to electron diffusion, and with the less realistic case of a perfect insulator, i.e the limit of very small conductivity.

We start by introducing the model. Taking a minimal set of balance equations to describe in fully a deterministic manner the discharge (see for example [8]), we will derive the contour dynamics equations for the evolution of the interface between the plasma region and the gas region free of charge (or with a very small density of charge). The outline of this derivation has already been reported [13] but here we present it in full details. Then, we proceed by studying a cylindrical discharge in the case of finite conductivity, and the analytical limits of infinite resistivity and ideal conductivity. With the model at hand we will predict some features of the stability of the fronts. Numerical simulations are made to calculate the dispersion curves and test some of the analytical predictions. We briefly describe the numerical methods employed in the corresponding section. Finally, we end with an analysis of results and overview of possibilities that the model opens for more complicated geometries and fully 3D cases.

II. THE DYNAMICAL CONTOUR MODEL

In this section we obtain our model as a limit of a set of balance equations describing a streamer discharge. We will first recall the minimal description of a streamer discharge and some of the properties of the traveling planar fronts, and then make use of the asymptotic

behaviour of those planar fronts in the limit of small diffusion to give a correction to the velocity of propagation of curved fronts. After finding the dynamics of the effective interface, a balance of the charge transport along the interface will be provided in order to complete the model.

A. The minimal model

For simulating the dynamical streamer development of streamers out of a macroscopic initial ionization seed, in a non-attaching gas like argon or nitrogen, the model of a streamer discharge [16] can be simplified. Attachment and recombination processes can be neglected as the probability or cross sections of such processes are much smaller than the ionization cross section in experimental data for non-attaching gases. We also ignore photoionization processes. With these considerations in mind, the resulting balance equations are

$$\frac{\partial N_e}{\partial t} = \nabla \cdot (\mu_e N_e \mathbf{E} + D_e \nabla N_e) + \nu_i N_e, \quad (3)$$

$$\frac{\partial N_p}{\partial t} = \nu_i N_e, \quad (4)$$

where N_e is the electron density, N_p is the positive ion density, μ_e is the electron mobility and D_e the diffusion coefficient. The ionization coefficient ν_i takes the phenomenological approximation suggested by Townsend, which leads to

$$\nu_i = \mu_e l_0^{-1} |\mathbf{E}| \exp\left(-\frac{E_0}{|\mathbf{E}|}\right), \quad (5)$$

where l_0 is the ionization length, and E_0 is the characteristic impact ionization electric field. Those parameters are determined by fitting experimental data [17]. Note also that $\mu_e \mathbf{E}$ is the drift velocity of electrons and it is assumed that the positive ions do not move which is a valid approximation at the initial stages of the streamers development. The model is completed by considering Gauss's law

$$\nabla \cdot \mathbf{E} = \frac{e(N_p - N_e)}{\epsilon_0}. \quad (6)$$

It is convenient to reduce the equations to dimensionless form. The Townsend approximation provides physical scales and intrinsic parameters of the model as long as only impact ionization is present in the gas [3]. In this case, the units are given by the ionization length l_0 , the characteristic impact ionization field E_0 , and the electron mobility μ_e , which lead to the

velocity scale $U_0 = \mu_e E_0$, and the time scale $\tau_0 l_0 / U_0$. Typical values of these quantities for nitrogen at normal conditions are $\alpha_0^{-1} \approx 2.3 \mu\text{m}$, $E_0 \approx 200 \text{ kV/m}$, and $\mu_e \approx 380 \text{ cm}^2/\text{Vs}$. We introduce the dimensionless variables $\mathbf{r}_d = \mathbf{r}/l_0$, $t_d = t/\tau_0$, the dimensionless field $\mathbf{E}_d = \mathbf{E}/E_0$, the dimensionless electron and positive ion particle densities $\rho_e = N_e/N_0$ and $\rho_p = N_p/N_0$ with $N_0 = \varepsilon_0 \mathcal{E}_0 / (el_0)$, and the dimensionless diffusion constant $D = D_e / (l_0 U_0)$. In terms of dimensionless variables, the model equations become

$$\frac{\partial n_e}{\partial t} = \nabla \cdot (n_e \mathbf{E} + D \nabla n_e) + n_e \alpha(|\mathbf{E}|), \quad (7)$$

$$\frac{\partial n_p}{\partial t} = n_e \alpha(|\mathbf{E}|), \quad (8)$$

$$\nabla \cdot \mathbf{E} = n_p - n_e, \quad (9)$$

$$\alpha(|\mathbf{E}|) = |\mathbf{E}| \exp(-1/|\mathbf{E}|), \quad (10)$$

where the subindex d has been dropped. The set of equations (7)–(10) is known as the minimal streamer model.

B. Planar fronts and boundary layer

Using the minimal streamer model, we can compute traveling wave solutions in the planar case. Those are solutions such as n_e and n_p decay exponentially at infinity. This means that we can take

$$\begin{aligned} n_e &= A e^{-\lambda(x-vt)}, \\ n_p &= B e^{-\lambda(x-vt)}, \\ \mathbf{E} &= (E^+ + C e^{-\lambda(x-vt)}) \hat{\mathbf{x}}, \end{aligned}$$

asymptotically far behind the planar wave in the $\hat{\mathbf{x}}$ direction. Introducing these expressions into (7) to (10), we obtain for $x - vt \rightarrow +\infty$, the relation

$$D\lambda^2 - (E^+ + v)\lambda + \alpha(|E^+|) = 0, \quad (11)$$

which has real solutions if and only if

$$v \geq -E^+ + 2\sqrt{D\alpha(|E^+|)}. \quad (12)$$

All initial data decaying at infinity faster than $Ae^{-\lambda^* x}$, with $\lambda^* = 1/\sqrt{D\alpha(|E^+|)}$, will develop traveling waves [3] with velocity $v^* = -E^+ + 2\sqrt{D\alpha(|E^+|)}$.

If $D \ll 1$ the profiles for n_p and \mathbf{E} will vary very little from the profiles with $D = 0$ and n_e will develop a boundary layer at the front. This boundary layer has a width of $O(\sqrt{D})$ as shown in [10]. The main results for the structure of the boundary layer which we are going to make use are

$$n_e = f(\chi), \quad (13)$$

$$n_p = -\sqrt{D} \int_{\chi}^{\infty} f(z) dz, \quad (14)$$

$$\mathbf{E} = \mathbf{E}^+ + \sqrt{D} \mathbf{E}_{bl} + O(D), \quad (15)$$

with $\chi = (x - v^*t)/\sqrt{D}$, and \mathbf{E} the electric field in the $\hat{\mathbf{x}}$ direction. The function $f(\chi)$, also appearing in (14), becomes the solution of a Fisher equation under the additional assumptions that the Townsend factor $\alpha(|\mathbf{E}|) \approx |\mathbf{E}|$ i.e. the electric field is large enough, and at the boundary layer $n_p \approx 0$ (details can be found in [10]).

C. The correction due to the curvature

Next we will add the correction to the propagation velocity due to the curvature of the front. We take a level surface of n_e representing the interface, and introduce local coordinates τ (along the level surfaces of n_e) and ν (orthogonal to the level surfaces of n_e). It is natural to scale the normal coordinate with the boundary layer thickness $\nu = \chi\sqrt{D}$, so that we can write

$$D \Delta = \frac{\partial^2}{\partial \chi^2} + \sqrt{D} \kappa \frac{\partial}{\partial \chi} + D \left(\Delta_{\perp} - \kappa^2 \chi \frac{\partial}{\partial \chi} \right) + O(D^{\frac{3}{2}}),$$

where $\Delta \equiv \nabla^2$ is the Laplacian operator, Δ_{\perp} is the transverse Laplacian and κ is twice the mean curvature in 3-D or just the curvature in 2-D (see e.g. [20]). Hence from (7) and (9)

$$\begin{aligned} \frac{\partial n_e}{\partial t} - \mathbf{E}_{\tau} \frac{\partial n_e}{\partial \tau} - \left(\frac{\mathbf{E}_{\nu}}{\sqrt{D}} + \sqrt{D} \kappa \right) \frac{\partial n_e}{\partial \chi} - \frac{\partial^2 n_e}{\partial \chi^2} &= \\ &= n_e \alpha(|\mathbf{E}|) + n_e (n_p - n_e) + O(D). \end{aligned}$$

At the diffusive boundary we expand now $|\mathbf{E}|$ and n_p using the expressions (13)–(15) (as explained in [9] and [10]), so it is straightforward to end with

$$\frac{\partial n_e}{\partial t} - \mathbf{E}_{\tau} \frac{\partial n_e}{\partial \tau} - \left(\frac{\mathbf{E}_{\nu}}{\sqrt{D}} - 2\sqrt{\alpha(|\mathbf{E}_{\nu}|)} + \sqrt{D} \kappa \right) \frac{\partial n_e}{\partial \chi} = O(D^{\frac{1}{2}}), \quad (16)$$

where a curvature term appears and is relevant provided $1 \ll \kappa \ll D^{-\frac{1}{2}}$.

Eq. (16) is a transport equation for the electron density with velocity

$$\mathbf{v} = -\mathbf{E} + (2\sqrt{D\alpha(|\mathbf{E}|)} - D\kappa)\mathbf{n}, \quad (17)$$

so that the level line of n_e that we have chosen to describe the evolution of the interface moves with a normal velocity

$$v_N = -E_\nu + 2\sqrt{D\alpha(|\mathbf{E}|)} - D\kappa. \quad (18)$$

Notice that the level lines concentrate in a small region where n_e presents a jump from its bulk value to zero, so most level lines follow (18). Note also that the tangential velocity does not change the geometry of the curve during its evolution. Nevertheless, tangential exchanges of charge affect the evolution through the dependence of v_N on E_ν . The mathematical description of these will be the subject of next section.

D. Charge transport along the interface

In order to describe the charge transport along the interface we trace a “pillbox” \mathcal{D} around a surface element. The region \mathcal{D} will be such that $\Delta\tau \gg \Delta\nu$ and will contain both the diffusive layer for n_e and the region where the total negative charge density, i.e $n_e - n_p$, has significant values.

If we subtract (7) from (8) and integrate over \mathcal{D} we find

$$\begin{aligned} \frac{\partial}{\partial t} \int_{\mathcal{D}} (n_e - n_p) dV &= \int_{\partial\mathcal{D}} (n_e \mathbf{E} + D \nabla n_e) \cdot \mathbf{n} dS = \\ &= n_e E_\nu \Delta\tau \Big|_{\chi=-\infty}^{\infty} + O(D^{\frac{1}{2}}), \end{aligned} \quad (19)$$

where we have used that $n_e \rightarrow 0$ for $\chi = \nu/\sqrt{D} \gg 1$, $|\nabla n_e| \rightarrow 0$ for $|\chi| \gg 1$ and we have neglected the contributions of the lateral transport of charge by E_τ in comparison with exchange of charge with the bulk by E_ν . This assumption is also common in the Taylor-Melcher model and we will follow it.

Futhermore notice that

$$\frac{\partial}{\partial t} \int_{\mathcal{D}} (n_e - n_p) dV = \frac{\partial}{\partial t} \int_{-\infty}^{\infty} (n_e - n_p) \Delta\tau d\nu = \frac{\partial}{\partial t} (\sigma \Delta\tau), \quad (20)$$

and the length (or area) element of the surface will suffer a change during interface deformation given by

$$\frac{\partial \Delta\tau}{\partial t} = \kappa v_N \Delta\tau, \quad (21)$$

so that we can finally write the equation

$$\frac{\partial \sigma}{\partial t} + \kappa v_N \sigma = -\frac{E_\nu^-}{\varrho}, \quad (22)$$

where ϱ is the effective resistivity of the medium, given in this case as $\varrho^{-1} = \lim_{\chi \rightarrow -\infty} n_e$ and E_ν^- is the normal component of the electric field when approaching the interface from inside the plasma region. There is a jump in the normal component of the electric field across the interface given by

$$E_\nu^+ - E_\nu^- = -\sigma, \quad (23)$$

with E_ν^+ the normal component of the electric field when approaching the interface from outside the plasma region.

We can also include a source (an insulated wire inside the plasma, for instance at \mathbf{x}_0 , carrying a electric current $I(t)$). This source will create a current density inside the plasma and, since quasineutrality is fulfilled, we will have at the interior of Ω

$$\nabla \cdot \mathbf{j} = I(t)\delta(\mathbf{x} - \mathbf{x}_0). \quad (24)$$

By adding this contribution to (22) we can finally write

$$\frac{\partial \sigma}{\partial t} + \kappa v_N \sigma = -\frac{E_\nu^-}{\varrho} - j_\nu^-, \quad (25)$$

where j_ν^- is the current density coming from the ionized region Ω to its boundary $\partial\Omega$ in the normal direction ν .

E. The effective contour model

The Eqs. (18) and (25) together constitute the dynamical model able to describe the evolution of an interface separating a plasma region from a neutral region that we mentioned at the introduction.

Notice that in the case $\varrho^{-1} \gg 1$, we arrive to Lozansky-Firsov model [15] with a correction due to electron diffusion, meanwhile in the limit $D = 0$ we arrive at the classical Hele-Shaw model. Such a model is known to possess solutions that develop singularities in the form of cusps in finite time [18] but, when regularized by surface tension corrections, the interface may develop various patterns including some of fractal-type (see [19] for a recent development and references therein).

Eq. (2) will provide the surface charge density σ as a function of time. From it, we can compute the electric field and move the interface with (18). Two limits can be easily identified in the case of there is no charge injection inside the plasma, i.e $j_\nu^- \approx 0$: a) the limit of large conductivity

$$\varrho^{-1} \gg 1, \quad E_\nu^- = 0,$$

so that the interface is equipotential and b) the limit of small conductivity

$$\varrho^{-1} \ll 1, \quad \frac{\partial}{\partial t}(\sigma \Delta \tau) = 0 \Rightarrow \sigma \Delta \tau = C,$$

where the charge contained by a surface element is constant and the density only changes through deformation (with change of area) of the interface. In the next sections we will study the intermediate case of finite resistivity.

III. THE CASE OF FINITE RESISTIVITY IN 2-D GEOMETRIES

As an application we will solve the 2-D case for different conductivities. In order to grasp some features of the model first we will consider how fronts with radial symmetry evolve. Then we will study the stability of those fronts under small perturbations and finally we will solve the model numerically in order to test some of the analytical predictions.

A. Solutions with radial symmetry

The electric potential created by a surface charge distribution with radial symmetry at the distance r is found by solving the equation

$$\Delta V = \sigma \delta(r). \tag{26}$$

The fundamental solution turns out to be in polar coordinates

$$V(\mathbf{x}) = \begin{cases} C \log |\mathbf{x}|, & |\mathbf{x}| > r \\ C \log r, & |\mathbf{x}| \leq r \end{cases} \tag{27}$$

where C will be determined by the condition of the electric field jump (23) at the surface. From the potential solution we can compute the electric field which has a discontinuity at the surface

$$E_\nu^- = 0, \quad E_\nu^+ = -\frac{C}{r}. \tag{28}$$

For the current density, the solution of (24) gives

$$\mathbf{j} = \frac{I(t)}{2\pi r^2} \mathbf{r}, \quad (29)$$

and finally using (2) and the fact that $v_N = dr/dt$ and $\kappa = 1/r$, we get

$$\frac{\partial \sigma}{\partial t} + \frac{1}{r} \frac{\partial r}{\partial t} \sigma = -\frac{I(t)}{2\pi r}. \quad (30)$$

This equation can be easily solved. We can write it as

$$\frac{\partial(r\sigma)}{\partial t} = -\frac{I(t)}{2\pi}, \quad (31)$$

to get

$$\sigma = -\frac{Q(t)}{2\pi r}, \quad \text{with} \quad Q(t) = \int_0^t I(t) dt, \quad (32)$$

where we have assumed that $\sigma(0) = 0$. Now we can see from the condition (23) that $C = -Q(t)/2\pi$, so

$$E_\nu^+ = \frac{Q(t)}{2\pi r}. \quad (33)$$

Then, defining $\varepsilon \equiv D$, the interface evolves according to (1) as

$$\frac{dr}{dt} = -\left(\frac{Q(t)}{2\pi} + \varepsilon\right) \frac{1}{r} + 2\sqrt{\varepsilon\alpha(|Q(t)/2\pi r|)}. \quad (34)$$

We shall analyze next two limiting cases. First the case where

$$r \ll \frac{|Q(t)|}{4\pi\varepsilon^{\frac{1}{2}}\sqrt{\alpha(|Q(t)/2\pi r|)}}, \quad \text{and} \quad \varepsilon \ll 1. \quad (35)$$

Then expression (34) results

$$\frac{dr}{dt} \approx -\frac{Q(t)}{2\pi r}, \quad (36)$$

so

$$r(t) \approx \sqrt{r(0)^2 - \int_0^t Q(t')/\pi dt'}. \quad (37)$$

For the particular case $Q(t) = Q$ is constant

$$r(t) \approx \sqrt{r(0)^2 - tQ/\pi} \quad (38)$$

The second case is the opposite one. If

$$r \gg \frac{|Q(t)|}{4\pi\varepsilon^{\frac{1}{2}}\sqrt{\alpha(|Q(t)/2\pi r|)}}, \quad \text{and} \quad \varepsilon \ll 1, \quad (39)$$

we have now

$$\frac{dr}{dt} \approx 2\varepsilon^{\frac{1}{2}} \sqrt{\alpha(|Q(t)/2\pi r|)}. \quad (40)$$

For the particular case $Q(t) = Q$, by standard asymptotic calculations, when $t \gg 1$ we deduce

$$r(t) \approx \frac{|Q|}{\pi} \log t. \quad (41)$$

B. Stability analysis

We will study now the stability of the fronts under small perturbations. We change by a small amount the position of the front as well as the charge density. The perturbed position and charge surface density of the interface on the interface will be parametrized using the polar angle as

$$r(\theta, t) = r(t) + \delta S(\theta, t), \quad (42)$$

$$\sigma(\theta, t) = -\frac{Q(t)}{2\pi r(\theta, t)} + \delta \Sigma(\theta, t), \quad (43)$$

where $r(t)$ is the solution of the equations for the radial symmetrical front, $Q(t) = \int_0^t I(t) dt$ and δ will be our bookkeeping small parameter for the expansions that follow.

We will start calculating the correction to the electric field due to the geometrical perturbation of the surface and the extra charge deposited on it. The electric potential will be, up to $O(\delta)$ order,

$$\Phi(\mathbf{x}) = V(\mathbf{x}) + \delta V_p(\mathbf{x}),$$

being V the solution for the symmetrical problem. The term $V_p(\mathbf{x})$ will satisfy the equation $\Delta V_p = O(\delta)$. Next we change coordinates to

$$\mathbf{x} \longrightarrow \tilde{\mathbf{x}} = \mathbf{x} \frac{r(t)}{r(\theta, t)},$$

so the perturbed surface becomes a disk of radius $r(t)$. At zero order V_p satisfies the Laplace equation outside the disk. Hence we have in the new polar coordinates the solution

$$V_p(\tilde{r}, \theta) = \begin{cases} \sum_1^\infty \psi_n \cos(n\theta) \left(\frac{\tilde{r}}{r}\right)^n, & \tilde{r} > r \\ \sum_1^\infty \varphi_n \cos(n\theta) \left(\frac{\tilde{r}}{r}\right)^n, & \tilde{r} \leq r \end{cases} \quad (44)$$

where we have imposed the conditions of V_p remains finite at the origin and becomes zero at very large distances.

In the original variables \mathbf{x} the potential at the surface position coming from the exterior is

$$\begin{aligned}\Phi(\mathbf{x}_s^+) &= V(\mathbf{x}_s^+) + \delta V_p(\mathbf{x}_s^+) = \\ &= -\frac{Q(t)}{2\pi} \log(r + \delta S) + \delta V_p(\mathbf{x}_s^+) = \\ &= -\frac{Q(t)}{2\pi} \left(\log(r) + \delta \frac{S}{r} \right) + \delta V_p(\mathbf{x}_s^+) + O(\delta^2),\end{aligned}\tag{45}$$

and from the interior is

$$\Phi(\mathbf{x}_s^-) = V(\mathbf{x}_s^-) + \delta V_p(\mathbf{x}_s^-) = C(r, t) + \delta V_p(\mathbf{x}_s^-),\tag{46}$$

where $r = r(t)$ is the evolving radius of the unperturbed circle, i.e. the radially symmetric solution of equations (1) and (2).

Now imposing the condition of continuity for the potential, we have

$$V_p(\mathbf{x}_s^+) = V_p(\mathbf{x}_s^-) + S \frac{Q(t)}{2\pi r(t)},$$

and if we write the surface perturbation as

$$S = \sum_{n=1}^{\infty} s_n(t) \cos(n\theta),\tag{47}$$

we find that the coefficients of the potential in (44) are related by

$$\psi_n = \varphi_n + \frac{Q(t)}{2\pi r} s_n.\tag{48}$$

Let us calculate the electric field to δ order. Making use of the expressions (44)–(48), and changing back coordinates from $\tilde{\mathbf{x}}$ to \mathbf{x} , the normal components of the electric field at both sides of the surface are

$$\begin{aligned}E_\nu^+ &= \frac{Q(t)}{2\pi(r + \delta S)} + \delta \sum_1^{\infty} \left(\varphi_n + \frac{Q(t)}{2\pi r} s_n \right) \frac{n}{r} \cos(n\theta), \\ E_\nu^- &= -\delta \sum_1^{\infty} \varphi_n \frac{n}{r} \cos(n\theta).\end{aligned}\tag{49}$$

Then, the jump condition (23) together with (43) give the following expression for the charge perturbation

$$\Sigma = - \sum_{n=1}^{\infty} \left(2\varphi_n + \frac{Q(t)}{2\pi r} s_n \right) \frac{n}{r} \cos(n\theta).\tag{50}$$

We still need the expression of the curvature up to δ order to find the dynamics of the front. In polar coordinates, after introducing the perturbation (42), the curvature turns out to be

$$\kappa = \frac{r^2 + 2rS\delta - rS_{\theta\theta}\delta + O(\delta^2)}{(r^2 + 2rS\delta + O(\delta^2))^{\frac{3}{2}}} = \frac{1}{r} - \frac{S + S_{\theta\theta}}{r^2}\delta + O(\delta^2), \quad (51)$$

and the normal component of the velocity

$$v_N = \mathbf{v} \cdot \mathbf{n} = \frac{dr(t)}{dt} + \delta \frac{\partial S(\theta, t)}{\partial t}. \quad (52)$$

The contour model equation (1), after introducing the perturbations to first order gives

$$\begin{aligned} \frac{dr(t)}{dt} + \delta \frac{\partial S(\theta, t)}{\partial t} &= -\frac{Q(t)}{2\pi r} + \delta S \frac{Q(t)}{2\pi r^2} - \delta \sum_1^{\infty} \left(\varphi_n + \frac{Q(t)}{2\pi r} s_n \right) \frac{n}{r} \cos(n\theta) + 2\varepsilon^{\frac{1}{2}} \sqrt{\alpha_0 + \delta\alpha_1} - \\ &- \varepsilon \left(\frac{1}{r} - \delta \frac{S + S_{\theta\theta}}{r^2} \right). \end{aligned} \quad (53)$$

Now, from (10) we have

$$\alpha_0 + \delta\alpha_1 = |E_0 + \delta E_1| e^{-\frac{1}{|E_0 + \delta E_1|}} = |E_0| e^{-\frac{1}{|E_0|}} + \delta \operatorname{sign}(E_0) E_1 \left(1 + \frac{1}{|E_0|} \right) e^{-\frac{1}{|E_0|}},$$

where, using (49),

$$E_0 = \frac{Q(t)}{2\pi r}, \quad (54)$$

$$E_1 = \sum_{n=1}^{\infty} \left(n\varphi_n + (n-1) \frac{Q(t)}{2\pi r} s_n \right) \frac{1}{r} \cos(n\theta), \quad (55)$$

so that

$$\sqrt{\alpha} = \sqrt{\alpha_0} + \delta \frac{\alpha_1}{2\sqrt{\alpha_0}} = \sqrt{\alpha_0} \left[1 + \delta \operatorname{sign}(Q(t)) \frac{E_1}{2|E_0|} \left(1 + \frac{1}{|E_0|} \right) \right].$$

Taking into account (34) for the zero order term, we get from (53)

$$\frac{\partial S}{\partial t} = S \frac{Q(t)}{2\pi r^2} - \sum_1^{\infty} \left(\varphi_n + \frac{Q(t)}{2\pi r} s_n \right) \frac{n}{r} \cos(n\theta) + \varepsilon \left(\frac{S + S_{\theta\theta}}{r^2} \right) + \varepsilon^{\frac{1}{2}} \frac{\alpha_1}{\sqrt{\alpha_0}}, \quad (56)$$

and finally making use of the expansion (47) for the perturbation S yields

$$\begin{aligned} \frac{ds_n}{dt} &= \left[-1 + \varepsilon^{\frac{1}{2}} \frac{2\pi r \sqrt{\alpha_0} \operatorname{sign}(Q(t))}{|Q(t)|} \left(1 + \frac{2\pi r}{|Q(t)|} \right) \right] \frac{n}{r} \varphi_n - \\ &- \left[\frac{Q(t)}{2\pi r^2} (n-1) + \frac{\varepsilon}{r^2} (n^2 - 1) + \varepsilon^{\frac{1}{2}} \frac{(n-1) \sqrt{\alpha_0}}{r} \left(1 + \frac{2\pi r}{|Q(t)|} \right) \right] s_n. \end{aligned} \quad (57)$$

In order to find the correction to the charge density we take Eq.(2) and multiply it by $r(\theta, t)$. Then we use the curvature expansion (51) written as

$$\kappa = \frac{1}{r} - \frac{S}{r^2}\delta - \frac{S_{\theta\theta}}{r^2}\delta = \frac{1}{r(\theta, t)} - \frac{S_{\theta\theta}}{r^2}\delta,$$

where as we mentioned before $r = r(t)$ is the zero order term in the position, and the fact that

$$v_N = \frac{dr(\theta, t)}{dt}.$$

Hence

$$\frac{\partial(r(\theta, t)\sigma(\theta, t))}{\partial t} - r(\theta, t)\frac{S_{\theta\theta}}{r^2}v_N\sigma(\theta, t)\delta = -\frac{r(\theta, t)}{\varrho}E_\nu^- - \frac{I(t)}{2\pi},$$

so that, at $O(\delta)$,

$$\frac{\partial(r\Sigma)}{\partial t} + \frac{S_{\theta\theta}}{r}\frac{Q(t)}{2\pi r}\frac{dr}{dt} = \frac{1}{\varrho}\sum_1^\infty n\varphi_n \cos(n\theta). \quad (58)$$

Making use of the (34), (47) and (50), we get

$$-\frac{d}{dt}\left(2n\varphi_n + n\frac{Q(t)}{2\pi r}s_n\right) = \frac{Q(t)}{2\pi r^2}\frac{dr}{dt}n^2s_n + \frac{n}{\varrho}\varphi_n,$$

or after simplifying

$$2\frac{d\varphi_n}{dt} + \frac{Q(t)}{2\pi r}\frac{ds_n}{dt} = -\frac{Q(t)}{2\pi r^2}\frac{dr}{dt}(n-1)s_n - \frac{I(t)}{2\pi r}s_n - \frac{1}{\varrho}\varphi_n.$$

Finally, using (34) and (57)

$$\begin{aligned} & 2\frac{d\varphi_n}{dt} + \frac{Q(t)}{2\pi r}\left[-\frac{n}{r}\varphi_n + \varepsilon^{\frac{1}{2}}\frac{2\pi r\sqrt{\alpha_0}\text{sign}(Q(t))}{|Q(t)|}\left(1 + \frac{2\pi r}{|Q(t)|}\right)\frac{n}{r}\varphi_n - \right. \\ & \left. -\frac{Q(t)}{2\pi r^2}(n-1)s_n - \frac{\varepsilon}{r^2}(n^2-1)s_n - \varepsilon^{\frac{1}{2}}\frac{(n-1)\sqrt{\alpha_0}}{r}\left(1 + \frac{2\pi r}{|Q(t)|}\right)s_n\right] =, \\ & = -\frac{Q(t)}{2\pi r^2}\left(-\frac{Q(t)}{2\pi r} - \frac{\varepsilon}{r} + 2\varepsilon^{\frac{1}{2}}\sqrt{\alpha_0}\right)(n-1)s_n - \frac{I(t)}{2\pi r}s_n - \frac{1}{\varrho}\varphi_n \end{aligned}$$

and after rearranging the terms

$$\begin{aligned} \frac{d\varphi_n}{dt} &= \frac{1}{2}\left[\frac{Q(t)}{2\pi r^2}n - \varepsilon^{\frac{1}{2}}\frac{n\sqrt{\alpha_0}}{r}\left(1 + \frac{2\pi r}{|Q(t)|}\right) - \frac{1}{\varrho}\right]\varphi_n + \\ & + \left\{\frac{Q(t)}{2\pi r^2}\left[\frac{Q(t)}{2\pi r} + \frac{(n+2)\varepsilon}{2r} + \varepsilon^{\frac{1}{2}}\sqrt{\alpha_0}\left(\frac{\pi r}{|Q(t)|} - \frac{1}{2}\right)\right](n-1) - \frac{I(t)}{4\pi r}\right\}s_n. \end{aligned} \quad (59)$$

Thus the time evolution of each particular mode has been obtained and it is governed by (57) and (59).

C. Special limits

First we study the limit of ideal conductivity. It corresponds to $\varrho \rightarrow 0$, and hence, from (59), we can conclude that $\varphi_n \rightarrow 0$. Physically this means that in the limit of very high conductivity, the electric field inside goes to zero ($E_\nu^- \rightarrow 0$), as we approach to the behavior of a perfect conductor. If we consider that $Q(t) = Q_0$ is constant or its variation in time is small compared with the evolution of the modes (which also implies $I(t) \rightarrow 0$), and the same for the radius of the front $r(t) = r_0$, we can try a solution $s_n = \exp(\omega_n t)$, $\varphi_n = 0$, to (57), and get a discrete dispersion relation of the form

$$\omega_n = -\frac{Q_0}{2\pi r_0^2}(n-1) - \frac{\varepsilon}{r_0^2}(n^2-1) - \varepsilon^{\frac{1}{2}} \frac{(n-1)\sqrt{\alpha_0}}{r_0} \left(1 + \frac{2\pi r_0}{|Q_0|}\right). \quad (60)$$

Next we consider the limit of finite resistivity, but such that the total charge is constant at the surface, or varies very slowly. Writing (59) as

$$\frac{d\varphi_n}{dt} = -\frac{d}{dt} \left(\frac{Q(t)}{4\pi r} s_n \right) - \frac{Q(t)}{4\pi r^2} \frac{dr}{dt} n s_n - \frac{1}{2\varrho} \varphi_n,$$

we have now

$$\frac{d\varphi_n}{dt} = -\frac{Q_0}{4\pi r_0} \frac{ds_n}{dt} - \frac{1}{2\varrho} \varphi_n. \quad (61)$$

For a small enough conductivity, $\varrho \rightarrow \infty$ so no extra charge reaches the surface, we find $\varphi_n = -\frac{Q_0}{4\pi r_0} s_n$, and with $s_n = \exp(\omega_n t)$, (57) yields

$$\omega_n = -\frac{Q_0}{2\pi r_0^2} \left(\frac{n}{2} - 1 \right) - \frac{\varepsilon}{r_0^2}(n^2-1) - \frac{\varepsilon^{\frac{1}{2}}\sqrt{\alpha_0}}{r_0} \left(1 + \frac{2\pi r_0}{|Q_0|}\right) \left(\frac{3n}{2} - 1 \right). \quad (62)$$

In a curved geometry we can see that the modes are discrete. However, if we compare (60) and (62), for small n and vanishingly small α_0 there is a 1/2 factor discrepancy in the dispersion curve between the two limits. In [21], the origin of this prefactor was discussed for planar fronts (the dispersion relation for planar fronts was obtained in the case of constant charge in [10]). So imposing constant charge at the surface, we get in this 2-D curved geometry case the same factor 1/2 that we got for the planar case. On the other hand, imposing constant potential at the surface gives a factor of 1. The intermediate situations can be studied by solving the system (57), (59).

Another consequence is that in both cases the maximum growth correspond to a perturbation with

$$n \propto |Q_0|/D, \quad (63)$$

provided that the $\varepsilon^{\frac{1}{2}}$ term can be neglected and Q_0 is negative, implying that the number of fingers increases with the net charge and decreases with electron diffusion.

D. Numerical simulations

In order to test the analytical predictions, we have calculated numerically the dispersion relation curves for the cases studied previously, when $\varrho \rightarrow 0$, so we have a perfect conducting plasma, and when ϱ remains finite. We will outline the numerical algorithms and we will show the results.

We start for the case of finite resistivity. The 2-D solution for the potential problem can be written as

$$\Phi(\mathbf{x}) = \int_C \frac{1}{2\pi} \log |\mathbf{x} - \mathbf{x}'| \sigma(\mathbf{x}') ds',$$

and the electric field results

$$\mathbf{E} = - \int_C \frac{1}{2\pi} \frac{\mathbf{x} - \mathbf{x}'}{|\mathbf{x} - \mathbf{x}'|^2} \sigma(\mathbf{x}') ds'.$$

In order to obtain the component in the normal direction E_ν , we will multiply it by the normal pointing outside the plasma region, i.e.

$$\mathbf{n} = \frac{(y_\alpha, -x_\alpha)}{\sqrt{x_\alpha^2 + y_\alpha^2}},$$

where the subindex denotes the derivative respect to the curve parameter α . So we can write

$$E_\nu = - \int_C \frac{1}{2\pi} \frac{(x - x', y - y')}{(x - x')^2 + (y - y')^2} \frac{(y_\alpha, -x_\alpha)}{\sqrt{x_\alpha^2 + y_\alpha^2}} \sigma(x', y') \sqrt{x_\alpha'^2 + y_\alpha'^2} d\alpha'.$$

Now when approximating the integral as a discrete sum on the interface, i.e. E_ν^+ limit, some care must be taken. We need the limit E_ν^+ on the curve. When \mathbf{x} coincides with \mathbf{x}' there is an extra contribution of half the pole, which is $\sigma(\mathbf{x})/2$. The E_ν^- can be obtained from the boundary condition (23), and the curvature will be expressed in the appropriate coordinates system.

The case of constant potential, which corresponds to $\varrho = 0$, is treated numerically as follows. We have to fulfill the condition

$$\int_C \frac{1}{2\pi} \log |\mathbf{x} - \mathbf{x}'| \sigma(\mathbf{x}') ds = V_0,$$

where V_0 is a constant for any \mathbf{x} belonging to C . Discretizing the domain in small segments S_i between points \mathbf{x}_i and \mathbf{x}_{i+1} we can approximate the integral as

$$\sigma(\bar{\mathbf{x}}_i) \int_{S_i} \frac{1}{2\pi} \log |\bar{\mathbf{x}}_i - \mathbf{x}'| ds + \sum_{\substack{j \\ i \neq j}} \frac{1}{2\pi} \log |\bar{\mathbf{x}}_i - \bar{\mathbf{x}}_j| \sigma(\bar{\mathbf{x}}_j) |\mathbf{x}_{j+1} - \mathbf{x}_j| = V_0,$$

where $\bar{\mathbf{x}}_i$ is the mean point of the S_i segment. The self contribution of the segment to the integral is taken as

$$\int_{S_i} \frac{1}{2\pi} \log |\bar{\mathbf{x}}_i - \mathbf{x}'| ds = \int_{-\frac{h_i}{2}}^{\frac{h_i}{2}} \frac{1}{2\pi} \log |x| dx = \frac{1}{2\pi} h_i \left(\log \frac{h_i}{2} - 1 \right),$$

being h_i the length of S_i . So we end with the equation

$$A_{ij} \sigma_j = V_0 \mathbf{1},$$

where $\mathbf{1}$ is the identity matrix, $\sigma_j = \sigma(\bar{\mathbf{x}}_j)$, and

$$A_{ij} = \begin{cases} \frac{1}{2\pi} h_j \log |\bar{\mathbf{x}}_i - \bar{\mathbf{x}}_j|, & \text{for } i \neq j \\ \frac{1}{2\pi} h_i \left(\log \frac{h_i}{2} - 1 \right), & \text{for } i = j \end{cases}$$

Due to the linearity of the problem, we can solve $A_{ij} \sigma_j = \mathbf{1}$ and do afterwards a further rescaling in order to fulfill $\sum \sigma_j h_j = Q$.

We will follow the evolution of a total initial dimensionless charge $Q = -10$ distributed uniformly along the curve given by

$$\begin{aligned} x(\theta) &= [1 + 0.05 \cos(n\theta)] \cos(\theta), \\ y(\theta) &= [1 + 0.05 \cos(n\theta)] \sin(\theta). \end{aligned} \tag{64}$$

where n gives the mode of the perturbation and θ is the curve parameter. We assume that there is not input current (so $j_v^- = 0$ in (2)), and then compute the exponential growth of each mode for a small period of time in order to get the dispersion curve. In Fig. 1, for different values of the inverse of the resistivity coefficient $1/\rho$ (or effective conductivity), we plot the corresponding dispersion curves.

Note that the slope increases with the increase of the conductivity of the plasma, the maxima moves to higher modes, and for larger n 's the dispersion curves become negative as predicted by (60) and (62). The slope around the origin $n = 1$ is larger for the case of ideal conductivity, i.e. when the interface is equipotential.

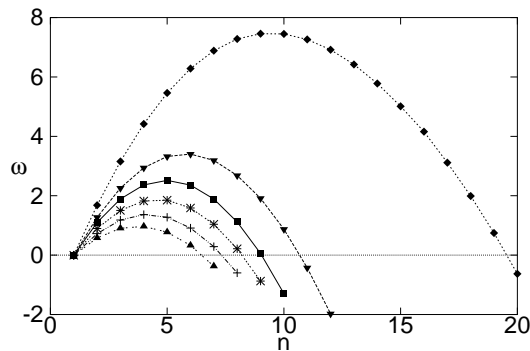


FIG. 1. Dispersion relation for the discrete modes of a perturbation with initial value $Q = -10$ for different inverse resistivities $1/\rho$. The \blacktriangle are for 0, $+$ for 5, $*$ for 10, \blacksquare for 15, \blacktriangledown for 25. The case of zero resistivity corresponds to \blacklozenge .

IV. CONCLUSIONS

We have presented the complete derivation of the contour dynamics model for electric discharges introduced in [13]. The model appears as the leading asymptotic description for the minimal streamer model when the electron diffusion coefficient is very small. It consists of two integro-differential equations defined at the boundary of the plasma region: one for the motion of the points of the boundary where the velocity in the normal direction is given in terms of the electric field created by the net charge there, and a second equation for the evolution of the charge density at the boundary. This second equation is very similar to the Taylor-Melcher model in electrohydrodynamics [14]. In the model the electric field is determined by solving Poisson equation with a given surface charge density, leading to a singular integral of the density.

Once our model has been deduced, we have computed explicit solutions with cylindrical symmetry and investigated their stabilities. The resulting dispersion relation is such as the perturbation with the small mode number can grow exponentially fast. In fact, both the number of modes become unstable and the mode that becomes most unstable (the one corresponding to the dispersion relation) depends critically on the electric resistivity of the media. We have computed analytically the dispersion relation and found that the number of unstable modes grows with the inverse of the resistivity (the conductivity) and the most unstable mode also increases with it. In the limit of vanishing resistivity one can consider

the medium as a perfect conductor and therefore impose that the potential is constant at the boundary. The dispersion relation for the model with finite resistivity converges to this limit when resistivity tends to zero.

We have implemented a numerical procedure to solve our model in general situations. In order to develop the numerical method, we needed to evaluate certain singular integrals that appear when computing the electrical field. As one result of the numerical method, the dispersion relations have been computed and compared them with the analytical results.

As a difference to our previous communication [13], we have paid special attention to the effects of Townsend expression for impact ionization (5) on the dispersion relation and the cases of intermediate resistivities. Townsend term only produces a small quantitative correction although the dispersion relations are qualitatively identical. We are now in the process to complete the fully 3-D case and extend these results to more general geometries.

The authors thank support from the Spanish Ministerio de Educación y Ciencia under projects AYA2009-14027-C05-04 and MTM2008-0325.

-
- [1] A. N. Lagarkov and I. M. Rutkevich, *Ionization waves in electric breakdown on gases* (Springer-Verlag, New York, 1994).
 - [2] I. M. Rutkevich, *Sov. J. Plasma Phys.* **15**, 844 (1989).
 - [3] U. Ebert, W. van Saarloos, and C. Caroli, *Phys. Rev. Lett.* **77**, 4178 (1996); *Phys. Rev. E* **55**, 1530 (1997).
 - [4] D. Tanaka, S. Matsuoka, A. Kumada and K. Hidaka, *J. Phys. D: Appl. Phys.* **42**, 075204 (2009).
 - [5] M. Arrayás, M. A. Fontelos, and J. L. Trueba, *Phys. Rev. E* **71**, 037401 (2005); *J. Phys. A* **39**, 7561 (2006).
 - [6] A. S. Kyuregyan, *Phys. Rev. Lett.* **101**, 174505 (2008)
 - [7] M. Arrayás, M. A. Fontelos and J.L. Trueba. *J. Phys. D: Appl. Phys* **39** 5176-5182 (2006)
 - [8] M. Arrayás, U. Ebert, W. Hundsdorfer, *Phys. Rev. Lett.* **88**, 174502 (2002).
 - [9] M. Arrayás, M. A. Fontelos, and J. L. Trueba, *Phys. Rev. Lett.* **95**, 165001 (2005).
 - [10] M. Arrayás, S. Betelú, M. A. Fontelos, and J. L. Trueba, *SIAM J. Appl. Math.* **68**, 1122 (2008).

- [11] S. K. Dhali and P. F. Williams, Phys. Rev. A **31**, 1219 (1985); J. Appl. Phys. **62**, 4696 (1987).
- [12] P. A. Vitello, B. M. Penetrante, and J. N. Bardsley, Phys. Rev. E **49**, 5574 (1994).
- [13] M. Arrayás, M.A. Fontelos, C. Jiménez, Phys. Rev. E **81**, 035401(R) (2010).
- [14] D. A. Saville, Annu. Rev. Fluid Mech. **29** 27–64 (1997).
- [15] E.D. Lozansky and O.B. Firsov, J. Phys. D: Appl. Phys. **6**, 976–981 (1973).
- [16] M. Arrayás, J. L. Trueba, Cont. Phys. **46** 265–276.(2005).
- [17] Y. P. Raizer, *Gas Discharge Physics* (Springer, Berlin 1991).
- [18] P. Ya. Polubarinova-Kochina, Dokl. Akad Nauk USSR **47**, no 4, 254.257 (1945) (in Russian).
- [19] S. Li, J. S. Lowengrub, J. Fontana, P. Palffy-Muhoray, Phys. Rev. Lett. **102**, 174501 (2009).
- [20] L.M. Pismen, *Patterns and Interfaces in Dissipative Dynamics*, Springer, where this expansion is explained.
- [21] M. Arrayás, M. A. Fontelos and J.L. Trueba. Phys. Rev. Lett. **101**, 139502 (2008).